General-Purpose Harmonic Balance Analysis of Nonlinear Microwave Circuits Under Multitone Excitation

VITTORIO RIZZOLI, MEMBER, IEEE, CLAUDIO CECCHETTI, ALESSANDRO LIPPARINI, AND FRANCO MASTRI

Abstract —**This paper describes a powerful software tool for the simulation of nonlinear microwave circuits under single- or multiple-frequency excitation. The program operates in a truly general-purpose fashion, both circuit topology and active devices equivalent circuits being arbitrarily established by the user at the data entry level. Built-in facilities based on the multidimensional Fourier transform allow a straightforward and unrestricted treatment of mixer and intermodulation problems. Application capabilities are illustrated by a number of practical examples.**

I. Introduction

THE STEADILY growing importance of nonlinear microwave CAD techniques is attested to by the considerable number of research teams who have been making contributions to this field in the recent technical literature. What is probably more important, attention is currently being devoted to this subject within U.S.-Government-sponsored research activities such as the MIMIC program [1]. The complexity of the nonlinear CAD problem certainly warrants such an extensive effort. In fact, while some basic aspects, for example the simulation of periodically driven circuits, are relatively well settled, others, such as general noise analysis, are for the most part still at the stage of theoretical investigation [2].

At present, a good deal of research activity is geared toward the development of efficient frequency-domain methods for nonlinear circuit analysis under multitone excitation. For many years this problem has been treated by a variety of approximate procedures (e.g., [3]–[7]) whose principal function was to limit as far as possible the computational resources (both memory occupation and CPU time) required to do the job. Now, however, large memories and powerful CPU's tend to be available even in relatively small-size systems (not to mention supercomputers), so that full nonlinear numerical approaches to the multitone problem are becoming increasingly attractive.

Within the general framework of harmonic balance (HB) techniques, several solution schemes are available, based on single- or multidimensional Fourier transformation. In Section II of this paper we present a brief review of such methods (at least, of the best known ones), and try to point out their suitability for implementation in a general-purpose CAD environment. This aspect is of primary importance from the engineering standpoint, since a definite need exists for general-purpose numerical tools allowing conceptual developments to be realized in the solution of real-world simulation and design problems.

A certain amount of work in this direction has already been carried out. User-oriented programs for the analysis and optimization of perodically driven circuits have long been in the literature [8]–[10], and more recently software tools for the treatment of quasi-periodic regimes have become available, even commercially [11]–[15]. This paper is mainly devoted to the presentation of a harmonic balance simulator, named LARSIM, which was developed at the University of Bologna (Italy) in a joint effort of several research teams. A unique feature of this program is that nonlinear circuit analysis under three-tone excitation is implemented here in a general-purpose format.

Section III of the paper is devoted to a discussion of the basic system choices that have led to the definition of the program structure as it is now. In Section IV we describe the algorithmic basis for the treatment of multiple-frequency inputs via the multidimensional Fourier transform. Finally, in Section V we present a set of numerical and experimental results giving a clear account of the vast potential of this software tool for microwave applications.

II. Multitone Analysis Algorithms

The problem of a circuit driven by a multiple-frequency input is one of fundamental importance for practical applications. Typical examples are mixer and intermodulation analysis. Since input power levels may be completely arbitrary, at least in principle, approximate approaches such as conversion-matrix techniques are not acceptable for a general-purpose simulator, and a full numerical solution must

Manuscript received April 6, 1988; revised August 31, 1988. This work was supported by the Italian Ministry of Education and by the Istituto Superiore delle Poste e delle Telecomunicazioni (ISPT).

V. Rizzoli and A. Lipparini are with the Dipartimento di Elettronica, Informatica e Sistemistica, University of Bologna, Bologna, Italy.
C. Cecchetti is with Fondazione U. Bordoni, Rome, Italy.
F. Mastri is with Fondazione G. Marconi, Villa Griffone, 40044 Pontecchio Marconi, Bologna, Italy.

IEEE Log Number 8824527.

0018-9480/88/1200-1650$01.00

be implemented. The main difficulty consists in finding the spectral components of the nonlinear subnetwork response to a multitone excitation. This problem has received a good deal of attention, and a number of solutions suitable for microwave applications are now available.

The simplest idea is to reduce the quasi-periodic regime to a strictly periodic one by taking the greatest common divider of the intermodulating tones as the fundamental frequency of operation, and then to use the fast Fourier transform. This approach has the obvious advantage of immediateness, since it allows any standard harmonic balance program to be used for mixer or intermodulation analysis; in fact it has been successfully applied by several authors in the technical literature (e.g., [16]–[18]). The main limitation arises from the fact that low values of the fundamental may lead to huge storage and CPU time requirements, which can easily exceed the available resources of even large supercomputers. This results in considerable restrictions on the combinations of input frequencies that are practically usable, which makes this choice unsuitable for a general-purpose simulator. It is quite clear that such limitations are due to the one-dimensional philosophy of the numerical method: when the fundamental is low, and thus the spectrum is very sparse, the required number of sampling points may far exceed the number of degrees of freedom of the signal waveforms; that is, the calculations performed are extremely redundant.

One way of strongly reducing such redundancy is to resort to *multidimensional* Fourier transformation [12]. Once again the basic idea is very simple: the instantaneous phase of each of the intermodulating signals is treated as an independent variable, so that the time-domain nonlinear subnetwork response becomes a multiple-periodic function (see Section IV). Time-domain sampling thus requires a multidimensional grid of sampling points, and conversion to the frequency domain can be performed by multiple Fourier transformation. The crucial point here is that the number of sampling points with respect to each of the independent time variables is related only to the maximum order of intermodulation products to be considered, and is not affected by the actual frequency values. The nice feature of this approach is that it can be implemented in a conventional harmonic balance program without any major change of the original program structure, and thus with little programming effort. Also, the subroutines for nonlinear device description are exactly the same, which is a considerable advantage for a user willing to employ his own device models.

The only drawback is that the grid sampling mechanism adopted still implies a certain degree of redundancy, which cannot be eliminated. To understand this point, let us consider a standard two-tone intermodulation (IM) problem. If all the IM products of two input frequencies ω_1, ω_2 up to a given order M are significant, any time-dependent electrical quantity may be given the form

$$x(t) = \sum_{k_1, k_2} X_{k_1, k_2} \exp\left[j(k_1\omega_1 + k_2\omega_2)t \right] \tag{1}$$

where

$$0 \leqslant |k_1| + |k_2| \leqslant M. \tag{2}$$

In this case the number of degrees of freedom of the signal is $2M^2 + 2M + 1$, but the two-dimensional Fourier approach requires a minimum of $(2M+1)^2$ sampling points, which is redundant by a factor of 2 (asymptotically for M large). Intuitively, (2) defines a triangular set of spectral lines, while the double Fourier transform requires a rectangular matrix of sampling points. Of course, the degree of redundancy depends on the truncation criterion adopted for the infinite summation (1).

Some analysis approaches allowing a nonredundant sampling are indeed available in the literature.

The matrix method described in [11] makes use of a number of sampling points exactly equal to the number of degrees of freedom of the signal waveforms. This leads to a system of linear equations for the output harmonics, which is solved to perform the transform. The sampling points must be suitably chosen in order to ensure that the system is well conditioned. The advantage of this approach is that a strictly nonredundant sampling is always carried out, no matter what the actual signal spectrum. The obvious drawback is that the algorithm performs a *conventional*, rather than a *fast* Fourier transform, in the sense that it does not take advantage of the well-established techniques for reducing the number of operations on which all FFT algorithms are based. This implies a consistent loss of numerical efficiency, so that this transform is usually slower than the multidimensional Fourier transform despite the reduced number of sampling points.

As an example, let us consider the IM problem defined by (1) and (2) with $M = 7$. This can be analyzed by a double FFT of size 16×16, requiring about 5.5 ms on a VAX 8800 (after initialization) by standard library routines. On the other hand, in this case the signal (1) has 113 degrees of freedom. Thus to carry out the same transform by the matrix method, one has to multiply a square matrix of order 113 by a vector of the same size. This takes about 20 ms on the VAX 8800. The difference is a growing function of the number of points.

A conceptually very attractive method is to carry out a one-dimensional Fourier analysis in a transformed frequency domain which is related to the physical one by a suitable mapping law [19]. In the transformed domain the exciting frequencies are chosen to be rationally independent with respect to an equivalent order of nonlinearity, corresponding to the maximum order of intermodulation products that are taken into account; this guarantees the frequency independence of the Fourier coefficients within the prescribed set of spectral lines. As a result, the original spectrum, having a few lines with large embedded gaps, is replaced by a transformed spectrum with drastically reduced gaps; in the standard IM problem defined by (1) and (2) the gaps are completely eliminated and the analysis is nonredundant. In exchange for its merits, this method is considerably more complex than the multidimensional FFT from the viewpoints of both program structure and nonlinear device description. This is particularly true in the three-tone case, since then the selection of the mapping law is not straightforward [19].

The methods of analysis discussed above have been demonstrated to be suitable for use within general-purpose programs for the simulation of nonlinear circuits under multiple-frequency excitation [11]–[14], [18], [19]. With the differences that have been pointed out, they share numerical accuracy, generality of application, and ease of implementation, and are thus most interesting from a practical viewpoint.

Of course, several other procedures have been developed for numerically solving the multitone problem. These include least-squares approximation [5], sampling at a reduced rate combined with linear superposition [4], [7], [20], and frequency shifting followed by digital filtering [21]. However, at least up to now, these approaches do not seem to have attained the degree of generality and maturity that the previous ones offer.

III. Available Options and Actual Choices for a Harmonic Balance Simulator

In this section we focus on the main "system choices" that have led to the present structure of the LARSIM program. There are many options available to anyone willing to develop a harmonic balance simulator, and different choices will result in profoundly different program architectures and performances. The topics to be discussed, which represent the cornerstones of any harmonic balance simulator, are listed below:

A. circuit analysis approach
B. nonlinear device description
C. evaluation of nonlinear device responses to a multitone excitation
D. nonlinear solution algorithm
E. gradient evaluation mechanism.

A. Circuit Analysis Approach

A very basic choice concerns the circuit analysis method. A common approach is to decompose the circuit into a linear and a nonlinear subnetwork having the same number of ports [22]. The linear subnetwork is analyzed in the frequency domain by conventional linear multiport techniques, while the nonlinear subnetwork is described in the time domain by a suitable set of device equations. Time- to frequency-domain conversion is provided by the fast Fourier transform. This is usually called a *piecewise* harmonic balance (PHB) technique, and is particularly convenient for the analysis of MMIC's when modern sophisticated modeling techniques are used in the linear subnetwork simulation [23]. In fact, when parasitics such as bends in transmission lines and other discontinuities are properly taken into account, the number of nodes of an MMIC usually becomes much larger than the number of subnetwork ports (often by an order of magnitude or more). Furthermore, in an MMIC each node is usually coupled to a considerable number of other nodes by a variety of mechanisms (such as proximity, radiation, and surface waves). Thus the node admittance matrix density is greatly increased, and sparse-matrix techniques [24] become considerably less attractive than for (say) hybrid circuits. An additional advantage of the PHB method is that the linear multiport analysis module may be directly replaced by any other with little interfacing effort. Thus the program may be easily updated by inserting into it new multiport analysis routines as soon as they become available. For these reasons the piecewise HB approach was adopted in LARSIM.

On the other hand, if most circuit nodes are connected with nonlinear devices, and the node admittance matrix is very sparse, this may not be the best choice. In such cases it may be convenient to use a nodal approach whereby the entire network is simultaneously described as a whole by means of Kirchhoff's current law, and all node voltages are automatically assumed as state variables [9]. However, for an MMIC this usually implies a much less refined simulation of the linear subnetwork, neglecting most junction parasitics and internodal couplings.

B. Nonlinear Device Description

The nonlinear subnetwork is usually a set of nonlinear devices which are best described by time-domain equations. A customary approach is to represent each device by a multiport parallel conductance/capacitance model. This means taking the voltages at the device ports as state variables and expressing each current as a memoryless function of such voltages plus the time derivative of another memoryless function of the same quantities (e.g., [9], [18], [25]). For increased generality we may remove the above constraints, and allow the state variables to be selected in a completely arbitrary way. In this case the voltages and currents at the device ports are expressed by a set of generalized parametric equations of the form [8]

$$\boldsymbol{v}(t)=\boldsymbol{u}\left[\boldsymbol{x}(t),\frac{d\boldsymbol{x}}{dt},\cdots,\frac{d^n\boldsymbol{x}}{dt^n},\boldsymbol{x}_D(t)\right]$$

$$\boldsymbol{i}(t)=\boldsymbol{w}\left[\boldsymbol{x}(t),\frac{d\boldsymbol{x}}{dt},\cdots,\frac{d^n\boldsymbol{x}}{dt^n},\boldsymbol{x}_D(t)\right] \quad (3)$$

where $\boldsymbol{u},\boldsymbol{w}$ are vector-valued nonlinear memoryless functions. In (3) $\boldsymbol{x}(t)$ represents the vector of time-dependent quantities used as state variables, and $\boldsymbol{x}_D(t)$ is a vector of time-delayed state variables, i.e.,

$$x_{D_i}(t)=x_i(t-\tau_i) \quad (4)$$

with τ_i representing a time constant. For well-conditioned devices the vectors appearing in (3) have a common size n_d, equal to the total number of device ports.

The use of (3) makes for increased ease and flexibility in the mathematical description of the nonlinear devices. As a typical example, we consider a microwave diode with a nonlinear series resistance depending on the junction voltage $x(t)$. A circuit model for such a diode is given in Fig. 1. If we take $x(t)$ as the (only) state variable, the diode

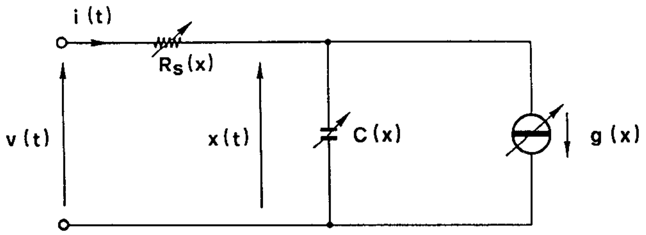

Fig. 1. Equivalent circuit of a microwave diode.

equations may be written in the form

$$i(t) = g[x(t)] + C[x(t)] \cdot dx/dt$$
$$v(t) = x(t) + R_S[x(t)] \cdot i(t). \tag{5}$$

In this case a simple description in terms of the external voltage $v(t)$ would be impossible.

The above approach was implemented in LARSIM for both library and user-defined device models.

C. Evaluation of Nonlinear Device Responses to a Multitone Excitation

For the reasons explained in Section II, the multidimensional Fourier transform approach [12] was adopted in LARSIM to evaluate the nonlinear subnetwork response to a multitone excitation. This method seemed to provide the best compromise between ease of programming, simplicity of user interaction, and numerical efficiency.

D. Nonlinear Solution Algorithm

When using the HB technique, a circuit simulation problem is mathematically formulated as a system of nonlinear algebraic equations of the form [10]

$$\boldsymbol{E}(\boldsymbol{X}) = \boldsymbol{0} \tag{6}$$

where $\boldsymbol{E}$ is a vector of HB errors to be evaluated numerically, and $\boldsymbol{X}$ is the set of all state-variable harmonics. A strategy for solving this system must be adopted by choosing among a large number of possible algorithms. The basic requirements are speed and robustness, which is intended here as the ability to reach the desired solution irrespective of the starting point. Unfortunately, these requirements are often conflicting, since robust algorithms tend to be slow and the converse is also true. As an example, relaxation methods are extremely fast when they work, but their convergence properties are poor [26]. System-solving algorithms such as the Newton iteration have a good overall performance, but still may fail to converge if the starting point is not close enough to the solution, especially in the case of highly nonlinear circuits. Nonlinear optimization algorithms are more robust, but become exceedingly slow in the vicinity of the solution [9].

A good tradeoff is to adopt a Newton iteration flanked by some other mechanism as a backup for improving convergence at startup whenever needed. A number of techniques were tried, including continuation methods [27], and the best results were obtained by a quasi-Newton method [28] based on a Hessian update formula of the Broyden family [29]. As a result, the solution algorithm implemented in LARSIM works as follows. In ill-conditioned cases the desired solution is first approached by the quasi-Newton algorithm; then automatic switchover takes place to a Newton iteration whereby the solution can be refined to any prescribed degree of accuracy. In well-conditioned cases the quasi-Newton iteration is bypassed. This allows the program to be successfully applied to a large number of different topologies including FET, bipolar-transistor, and multiple-diode circuits.

E. Gradient Evaluation Mechanism

The problem of derivative or gradient evaluation is obviously of importance for both the Newton and the quasi-Newton iteration. There are basically two options here: one is to compute the derivatives numerically by perturbations, that is, by a simple incremental rule. The other is to resort to a semi-analytic technique, which is possible if the Jacobians of (3) with respect to the state variables and to their time derivatives are available in closed form.

Let us consider a circuit excited by F independent sinusoidal tones of angular frequencies $\omega_1, \omega_2, \cdots, \omega_F$. A generic IM product will be identified by a vector $\boldsymbol{k}$ of harmonic numbers $k_1, k_2, \cdots, k_F$. The corresponding angular frequency will be denoted by

$$\omega_k = \sum_{\iota=1}^{F} k_\iota \omega_\iota = \boldsymbol{k}^T \boldsymbol{\omega} \tag{7}$$

where $\boldsymbol{\omega}$ is the vector of the fundamentals, and the superscript T denotes transposition. For any given state vector, the Jacobians of (3) may be represented by generalized Fourier series expansions. For example, for the currents at the device ports we may write

$$\frac{\partial \boldsymbol{w}}{\partial \boldsymbol{y}_m} = \sum_{\boldsymbol{k}} \boldsymbol{D}_{m,k} \exp(j\omega_k t)$$
$$\frac{\partial \boldsymbol{w}}{\partial \boldsymbol{x}_D} = \sum_{\boldsymbol{k}} \boldsymbol{D}'_{0,k} \exp(j\omega_k t) \tag{8}$$

where $\boldsymbol{y}_0 = \boldsymbol{x}$, $\boldsymbol{y}_m = d^m \boldsymbol{x}/dt^m$ $(1 \leqslant m \leqslant n)$. The summations in (8) are extended to all possible vectors $\boldsymbol{k}$. The Fourier coefficients appearing in (8) can be used to express the Jacobians of the current harmonics with respect to the state-variable harmonics in the form [10]

$$\frac{\partial \boldsymbol{W}_k}{\partial \boldsymbol{X}_s} = \sum_{m=0}^{n} (j\omega_s)^m \boldsymbol{\Delta}_{m,k-s} \tag{9}$$

where

$$\boldsymbol{\Delta}_{0,k-s} = \boldsymbol{D}_{0,k-s} + \boldsymbol{D}'_{0,k-s} \exp(-j\omega_s \boldsymbol{\tau})$$
$$\boldsymbol{\Delta}_{m,k-s} = \boldsymbol{D}_{m,k-s} \qquad (m > 0) \tag{10}$$

and $\boldsymbol{\tau}$ is the diagonal matrix of the time delays τ_ι appearing in (4).

For practical purposes, (6) is usually treated as a system of real equations in real unknowns, so that the real and imaginary parts of the state-variable harmonics become the actual problem unknowns. Since the state variables are real-valued ($X_{-k} = X_k^*$), from (9) we get

$$\frac{\partial W_k}{\partial [\mathrm{Re}(X_s)]} = \sum_{m=0}^{n} (j\omega_s)^m [\Delta_{m,k-s} + (-1)^m \Delta_{m,k+s}]$$
$$\frac{\partial W_k}{\partial [\mathrm{Im}(X_s)]} = \sum_{m=0}^{n} j(j\omega_s)^m [\Delta_{m,k-s} - (-1)^m \Delta_{m,k+s}]. \tag{11}$$

Similar expressions hold for the Jacobians of the voltage harmonics. From the above the Jacobians of the harmonic balance errors can be derived by trivial algebraic calculations.

The semianalytic method is faster and more accurate than the purely numerical approach, and is particularly convenient when simple and smooth device models are available, so that the analytic computation of the derivatives appearing on the left-hand side of (8) is easy and straightforward. On the other hand, many practical device models may be very complicated, may even be defined piecewise, resulting in cumbersome and sometimes ill-conditioned expressions of such analytic derivates. This can be annoying from the viewpoint of user interaction, particularly when user-defined device models have to be implemented. Once again, generality of application and ease of interaction were given preference in LARSIM by choosing to compute the Jacobians by the numerical approach.

IV. Algorithmic Aspects

Let the nonlinear subnetwork be described by (3), and let us consider a multitone excitation of the form

$$x(t) = \sum_k X_k \exp(j\omega_k t) \tag{12}$$

where the same notations introduced in Section III have been used. From (12) we get

$$\frac{d^m x}{dt^m} = \sum_k [(j\omega_k)^m X_k] \exp(j\omega_k t) \qquad (1 \leq m \leq n)$$
$$x_D(t) = \sum_k [X_k \exp(-j\omega_k \tau)] \exp(j\omega_k t) \tag{13}$$

where τ is the same diagonal matrix appearing in (10). In order to carry out a nonlinear circuit analysis by the harmonic balance technique, we have to compute the spectral components of the voltages and currents at the nonlinear subnetwork ports in the quasi-periodic electrical regime defined by (12). To do so, we treat the quantities

$$z_i = \omega_i t \qquad (1 \leq i \leq F) \tag{14}$$

appearing in (12) and (13) as independent variables, so that the state variables, their time derivatives, and their delayed values can be viewed as 2π-periodic functions of each z_i. Because of (3), the same is true for the voltages and currents. By Shannon's theorem, such functions are uniquely identified by the set of values they take at

$$\left.\begin{aligned} z_i &= (r_i - 1)\frac{2\pi}{N_i} \\ (1 &\leq r_i \leq N_i) \end{aligned}\right\} \qquad (1 \leq i \leq F) \tag{15}$$

where N_i is the number of sampling points in the z_i dimension, satisfying

$$N_i > 2K_i. \tag{16}$$

We denote by K_i the maximum value of k_i appearing in the expansion (12). Equation (15) defines an F-dimensional grid of sampling points.

Once a vector of state-variable harmonics (i.e., the set of all X_k's) has been selected in some way (e.g., by the generic step of an iterative solution algorithm), the coefficients of the expansions given by (13) are computed, and the values of (12) and (13) are sampled at all points defined by (15). Equations (3) then yield the sampled values of the voltages and currents, from which the required spectral components are obtained by performing an F-dimensional fast Fourier transform. The latter can always be reduced to a sequence of one-dimensional transforms, but can also be treated by means of highly efficient dedicated algorithms, at least in the two- and three-dimensional cases. As an example, the algorithm described in [30] allows FFT costs to be reduced by a factor of about 6 for $F = 3$ when run on a Cray X-MP computer in the typical case $N_1 = 16$, $N_2 = N_3 = 8$ (e.g., for mixer intermodulation analysis).

The remaining parts of the analysis are just a straightforward application of conventional harmonic balance principles [22].

The above algorithm has been implemented in LARSIM for $F \leq 3$, allowing full numerical analysis of arbitrary nonlinear circuits under two- and three-tone excitation. The program has facilities for the automatic determination of the spectral lines required in the commonly encountered cases of two- and three-tone IM analysis in general circuits, regular mixer analysis, and two-tone IM analysis in mixers.

Besides mixer IM analysis, an example of which is given in the next section, the three-tone capability opens the way to a systematic treatment of some very difficult problems for which general simulation methods have not been available until now. Among others we mention i) the analysis of a mixer pumped by a local oscillator having an internally generated spurious tone superimposed to the nominal output; ii) the determination of the spurious responses produced by a mixer under the effect of a strong input interfering signal; and iii) the computer-aided simulation of three-tone intermodulation tests, which are commonplace in the linearity evaluation of digital radio subsystems (especially for complex modulation formats). Work on these subjects is in progress, and the results will be reported elsewhere.

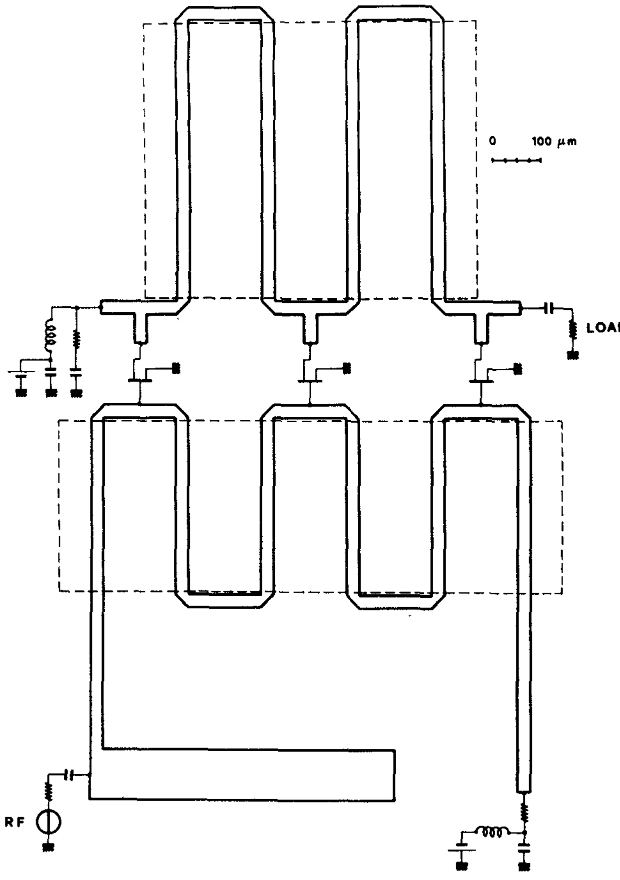

Fig. 2. Schematic topology of a three-FET distributed amplifier.

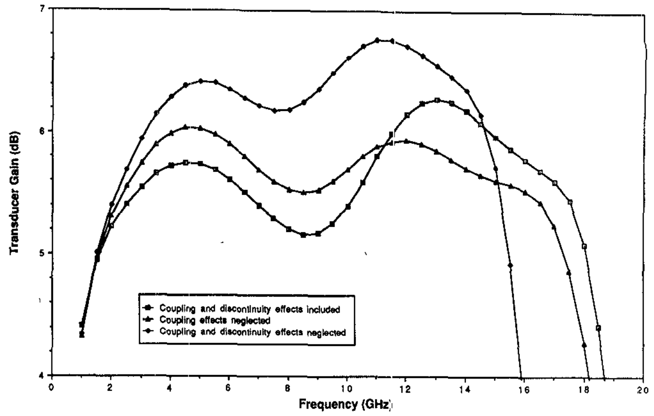

Fig. 3. Transducer gain of the distributed amplifier depicted in Fig. 2.

V. Numerical Examples

The purpose of this section is to illustrate the practical convenience and the far-reaching capabilities of multitone analysis software based on the principles outlined in the previous sections. This is done by discussing the application of LARSIM to a number of typical microwave engineering problems.

A. Distributed Amplifier of Realistic Topology

Let us consider the three-stage distributed amplifier whose layout is illustrated in Fig. 2. The FET's and the lumped components are shown schematically in this figure, but the layout of the microstrip circuitry is represented on scale. This circuit topology was obtained by reoptimizing the distributed amplifier described in [31] for a 150 μm GaAs substrate, with the additional constraint that the amplifier size should not exceed 1×1.5 mm. The FET small-signal equivalent circuit is the one given in [31]; the extension of the model to large-signal operation is accomplished by the equations described in [32].

The circuit contains a large number of microstrip discontinuities (T junctions and chamfered bends) which have a significant effect on its electrical performance. Furthermore, folding the microstrips to meet size requirements results in long sections of parallel transmission lines with edge-to-edge distances of 0.15 mm, whose electromagnetic couplings may not be neglected. Note that these couplings do not harm the amplifier performance (including stability), but must be accounted for in the optimization. Thus the sets of microstrips enclosed in the dashed lines in Fig. 2 must be treated as single circuit components with eight and 12 ports, respectively. For this purpose LARSIM makes available a lossy and dispersive coupled-microstrip model (up to 12 coupled lines) based on the spectral-domain approach [33]. The effects of couplings and parasitics on circuit performance are illustrated in Fig. 3, where the amplifier gain is plotted against frequency in the 1–19 GHz band. Neglecting couplings results in a 750 MHz reduction of the useful amplifier band, while neglecting couplings and parasitics leads to a band reduction of more than 3 GHz.

Two typical aspects of the computer-aided simulation of realistic GaAs topologies are clearly apparent from the above discussion. As a first point, the number of circuit nodes required by an accurate description, including parasitics, may be much larger than the number of device ports; e.g., for the simple amplifier of Fig. 2 the linear subnetwork has 75 nodes and six ports. Furthermore, due to coupling effects the circuit may include several components having large numbers of ports. This leads to the appearance of large, dense submatrices in the node admittance matrix. For instance, the node admittance matrix of the linear subnetwork for the amplifier of Fig. 2 contains one 8×8 and one 12×12 dense submatrix. It is clear that this kind of situation is best dealt with by the piecewise harmonic balance technique. For the circuit in Fig. 2, the PHB makes use of only six state variables and a 6×6 matrix to describe the linear subnetwork.

In order to give the reader an idea of the numerical performance of LARSIM, we report on a two-tone IM analysis of the distributed amplifier shown in Fig. 2. The two sinusoidal sources have an available power of 0 dBm each, and their frequencies f_1 and f_2 are swept across the amplifier band (i.e., from 2 to 18 GHz) while their difference is kept constant at 50 MHz. All IM products up to the third order are taken into account (12 spectral lines plus dc). The output powers at f_2, $f_1 + f_2$, and $2f_2 - f_1$ are plotted against frequency in Fig. 4. These results are generated by LARSIM in a single computer run. The

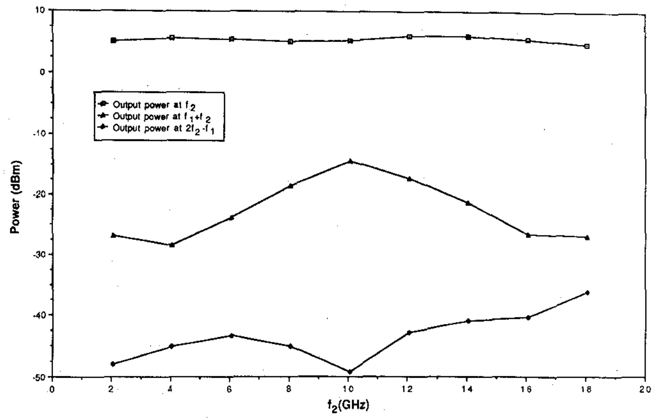

Fig. 4. Fundamental output power and IM products of the distributed amplifier depicted in Fig. 2.

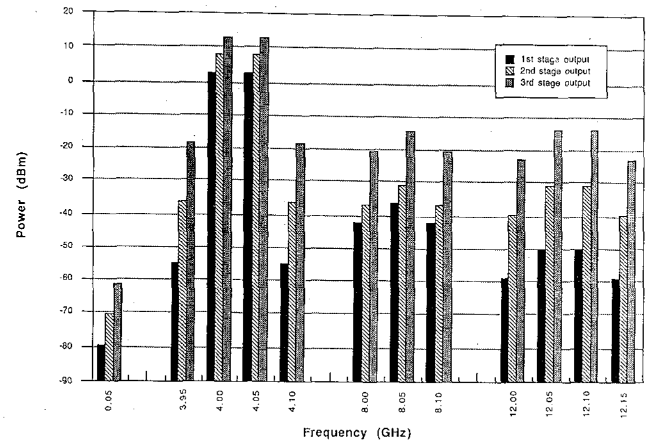

Fig. 5. Output power spectra of a three-stage, nine-FET distributed amplifier.

typical computational time is about 1.3 CPU seconds per frequency point on a Cray X-MP/48 using the vectorized version of LARSIM. Note that 37 percent of this time is spent in the linear subnetwork analysis.

As an example of a relatively large-size job, we consider a nine-FET amplifier consisting of the cascade connection of three units identical to the one shown in Fig. 2. This circuit is fed by two sinusoidal sources, each with an available power of -3 dBm, and having frequencies $f_1 = 4$ GHz and $f_2 = 4.05$ GHz. A two-tone intermodulation analysis is carried out with all IM products up to the third order taken into account. The power spectra of the output signals from the three stages of the cascade connection are shown in Fig. 5. These results are generated by LARSIM in a single computer run requiring about 48 CPU seconds on a Cray X-MP/48. The increased CPU time with respect to the previous analysis is partly due to a threefold increase in the number of Newton iterations required to achieve convergence. This is related to the higher power levels in the second and third stages. Note that this topology has as many as 219 circuit nodes; furthermore, its node admittance matrix contains three 8×8 and three 12×12 dense submatrices.

B. Large-Signal S Parameters

Large-signal circuit parameters (such as scattering or admittance parameters) of active devices are commonly used in several microwave engineering practices, for example, oscillator design (e.g. [34], [35]). It is thus interesting to establish a numerical procedure for extracting such parameters from any one of the well-known time-domain device models available in the technical literature. In this section we show that a multitone analysis program based on the multiple FFT, such as LARSIM, is ideally suited for this purpose.

For the sake of clarity, we refer to Fig. 6, where the common case of a biased FET is illustrated. A customary way of defining large-signal S parameters is as follows [34]. S_{11} and S_{21} are assumed to be functions of $|V_1|$ only, and are found from a circuit analysis with $E_2 = 0$. Similarly, S_{22} and S_{12} are assumed to be functions of $|V_2|$ only, and are found from a circuit analysis with $E_1 = 0$. A major drawback of this approach is that in the absence of *input* drive, the nonreciprocal active device works in an electrical regime substantially different from its real mode of operation. Thus S_{22} and S_{12} may be affected by a large error. This problem may be overcome by the "two-signal method" [36], that is, by simultaneously exciting the device with an input and an output source at the same frequency. The circuit is analyzed for several values of the phase difference between the two sources (and constant amplitudes), and the ratios between incident and reflected wave amplitudes at the two ports are monitored. On a Smith chart, these complex ratios approximately depict four circles whose centres are the large-signal S parameters [36].

As an example, let us assume that the intrinsic FET chip in Fig. 6 be described by the model of [37] with the following set of parameters:

$$\begin{aligned} V_T &= -3.2 \text{ V} & \beta &= 0.0178 \\ C_{GS0} &= 0.6 \text{ pF} & \lambda &= 0.0018 \\ V_{Bi} &= 0.8 \text{ V} & \alpha &= 1.71. \end{aligned} \tag{17}$$

The magnitude and phase of S_{22} as obtained from the two-signal method are plotted in Fig. 7 against the input available power for a fixed available power of the output source ($+12$ dBm). Note that S_{22} is approximately constant at low input signal levels, but starts to change rapidly as power saturation is approached (the 1-dB compression point for the circuit of Fig. 6 corresponds to an input power of $+18$ dBm). Thus the standard definition [34] may not be adequate in the case of power circuits.

The two-signal method is accurate and physically sound, but is practically cumbersome, since it requires many nonlinear analyses and a considerable amount of postprocessing of the computed data. As an alternative, we propose the following approach [38], which has the same degree of accuracy, but is much easier to implement. Assume that the S parameters have to be computed at a frequency f_1 as functions of the drive levels. A sinusoidal source of frequency f_1 having the prescribed power level is applied at the input port. At the output port we apply

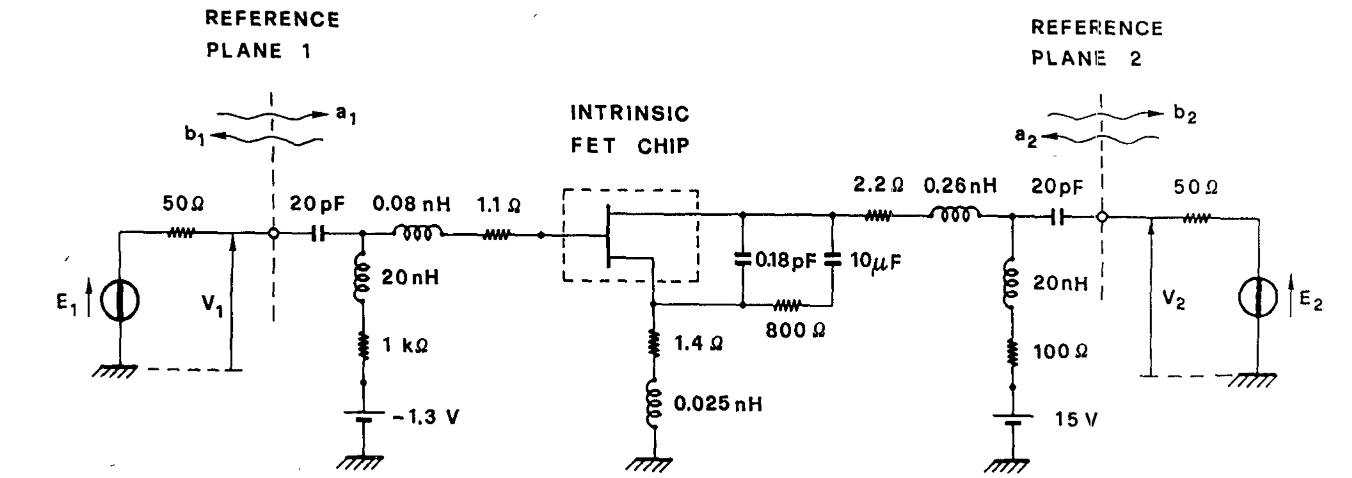

Fig. 6. Circuit schematic for computing the large-signal S parameters of a biased FET.

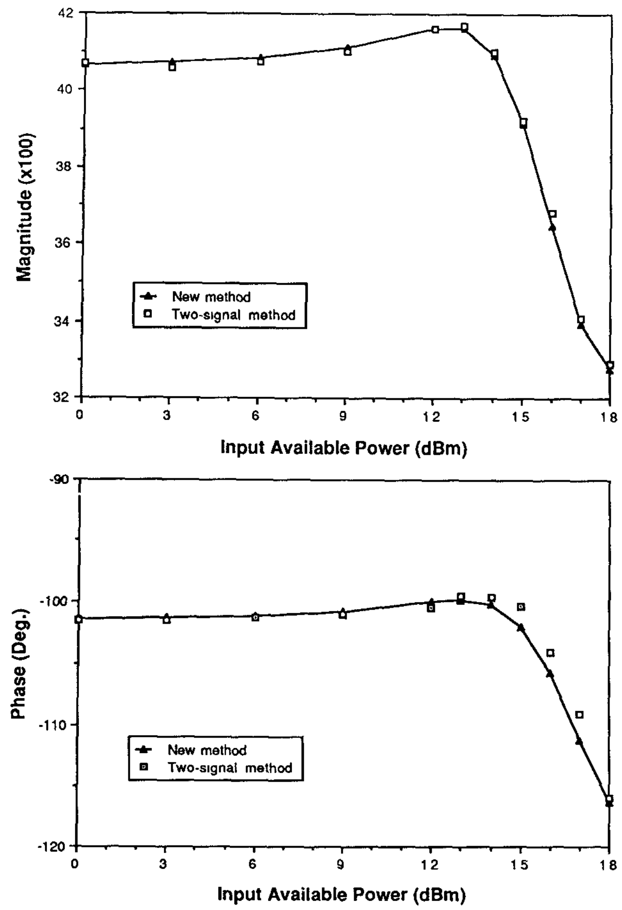

Fig. 7. Large-signal output reflection coefficient S_{22} of the biased FET depicted in Fig. 6 versus input available power.

another sinusoidal source having the prescribed output power level, but a frequency f_2 slightly different from f_1, e.g., $f_2 - f_1 = 10^{-4} f_1$. As a consequence, the device is operated in a quasi-periodic regime whose spectrum consists of the intermodulation products of f_1 and f_2 up to a given order (typically around 8 at high drive levels). If a two-tone analysis algorithm based on the two-dimensional Fourier transform is adopted, *infinite discrimination* between the two exciting signals is obtained no matter how close their

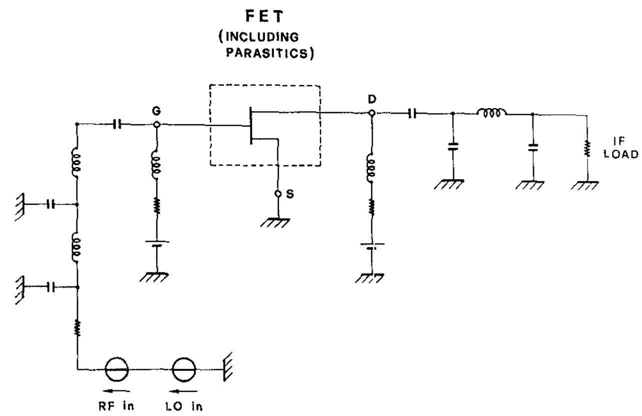

Fig. 8. Schematic topology of a broad-band FET gate mixer.

frequencies. Thus S_{11} and S_{21} can be obtained as b_1/a_1 and b_2/a_1 at f_1, and S_{22} and S_{12} are given by b_2/a_2 and b_1/a_2 at f_2. Since f_2 is very close to f_1, we can assume $S_{22}(f_1) = S_{22}(f_2)$ and $S_{12}(f_1) = S_{12}(f_2)$ with negligible error. A further simplification is possible when the large-signal S parameters are substantially independent of the power level of the output source E_2. There is experimental evidence that this should be approximately true in general, even in the case of highly nonlinear devices such as bipolar transistors operated in class C conditions [36]. With this assumption, E_2 can be set to a value much smaller than E_1 (e.g., $E_2 = 10^{-2} E_1$), so that a mixerlike spectrum can be used, with E_1 playing the role of "local oscillator" and E_2 that of "radio frequency." This reduces the number of spectral lines to be accounted for in the analysis (typically by a factor of 3), and makes convergence much easier to achieve.

The results of this analysis for the power FET shown in Fig. 6 are given in Fig. 7. The large-signal S parameters obtained in this way can be considered to be identical to those generated by the two-signal method of [36] for all practical purposes. Note that for the case considered the S parameters remain virtually unchanged when the available power of the output source is swept between -28 dBm and $+12$ dBm.

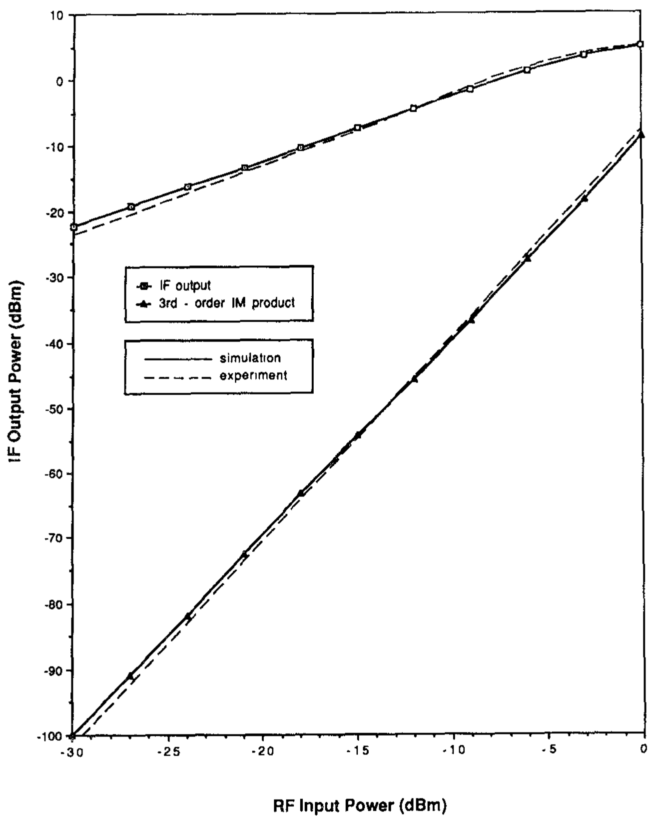

Fig. 9. Mixer IF output and near-carrier third-order IM product versus RF power for an LO power level of 5.7 dBm.

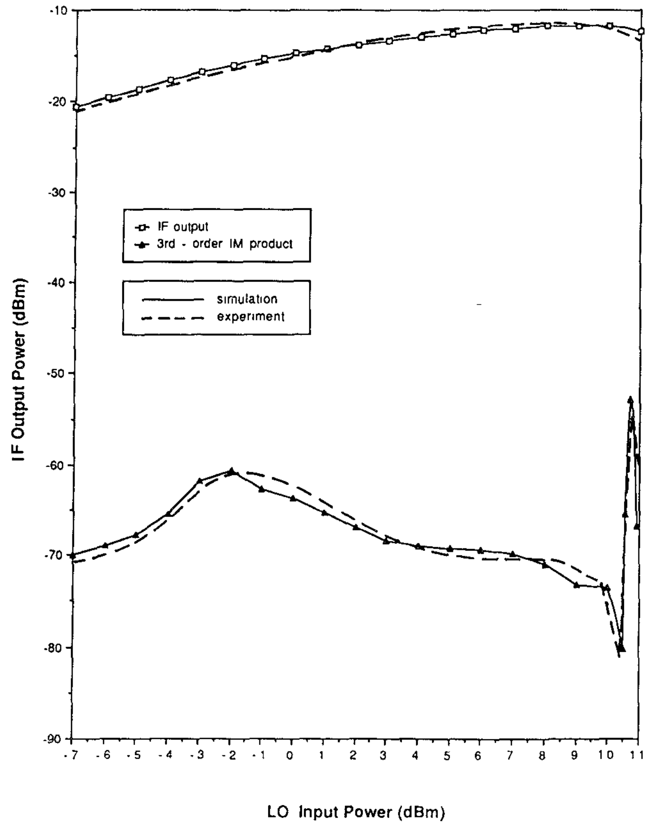

Fig. 10. Mixer IF output and near-carrier third-order IM product versus LO power for an RF power level of -20 dBm.

C. Two-Tone Intermodulation Distortion in a FET Mixer

As a final example of application, we consider the single-ended FET gate mixer whose topology is schematically depicted in Fig. 8. This mixer was designed for a conversion gain of 7.25 ± 0.25 dB and an input return loss of at least 13 dB over an IF band ranging from 100 to 1100 MHz [12], [13]. To analyze IM distortion, two RF signals of equal amplitudes are fed to the mixer input together with the LO. The frequency values considered are $f_1 =$ 8 GHz (LO), $f_2 = 8.50$ GHz, and $f_3 = 8.51$ GHz. Four LO harmonics and all IM products of the two RF signals up to the third order are taken into account, for a total of 112 frequencies plus dc. This analysis may be run in about 19 CPU seconds on a Cray X-MP/48. The results of this simulation are shown in Figs. 9 and 10. The quantities considered are the IF output $f_3 - f_1$ (510 MHz) and the down-converted third-order IM product $2f_3 - f_2 - f_1$ (520 MHz). These are plotted as functions of the RF input power in Fig. 9, and of the LO power in Fig. 10 (solid lines). From Fig. 9 the extrapolated third-order intercept point is found to be $+16.48$ dBm (IF output power—see [39] for reference). Fig. 10 shows the appearance of the typical sharp minima and maxima which have been experimentally observed in both passive and active microwave mixers [40]–[42].

A hybrid version of this mixer was built for demonstrational purposes using an AVANTEK AT-8251 device. The device equivalent circuit was derived from dc and scattering-matrix information by numerical optimization, following the method outlined in [32]. The fundamental device parameters are an I_{DSS} of about 100 mA, a zero-voltage barrier capacitance of 0.42 pF, and a pinch-off voltage of 2 V. The measured IF output and IM product are shown in Figs. 9 and 10 (dashed lines). The agreement with the computed results is found to be excellent: in particular, the local oscillator level yielding minimum near-carrier IM products can be predicted with high accuracy.

References

[1] M. R. Stiglitz, "GaAs technology and MIMIC, 1987," *Microwave J.*, pp. 42–47, Sept. 1986.

[2] V. Rizzoli and A. Neri, "State of the art and present trends in nonlinear microwave CAD techniques," *IEEE Trans. Microwave Theory Tech.*, vol. 36, pp. 343–365, Feb. 1988

[3] F. Filicori and C. Naldi, "An algorithm for the periodic or quasi-periodic steady-state analysis of non-linear circuits," in *1983 IEEE Int. Symp. Circuits Syst. Dig.* (Newport Beach), May 1983, pp. 366–369.

[4] R. J. Gilmore and F. J. Rosenbaum, "Modeling of nonlinear distortion in GaAs MESFETS," in *1984 IEEE MTT-S Int. Microwave Symp. Dig.* (San Francisco), June 1984, pp. 430–431.

[5] A. Ushida and L. O. Chua, "Frequency-domain analysis of nonlinear circuits driven by multi-tone signals," *IEEE Trans. Circuits Syst.*, vol. CAS-31, pp. 766–779, Sept. 1984.

[6] G. W. Rhyne and M. B. Steer, "Simulation of intermodulation distortion in MESFET circuits with arbitrary frequency separation of tones," in *1986 IEEE MTT-S Int. Microwave Symp. Dig.* (Baltimore), June 1986, pp. 547–550.

[7] J. Dreifuss, A. Madjar, and A. Bar-Lev, "A full large-signal analysis of active microwave mixers," in *Proc. 16th European Microwave Conf.* (Dublin), Sept. 1986, pp. 687–691.

[8] V. Rizzoli, A. Lipparini, and E. Marazzi, "A general-purpose program for nonlinear microwave circuit design," *IEEE Trans Microwave Theory Tech.*, vol. MTT-31, pp. 762–770, Sept 1983.

[9] K. S. Kundert and A. Sangiovanni-Vincentelli, "Simulation of nonlinear circuits in the frequency domain," *IEEE Trans. Computer-Aided Design*, vol. CAD-5, pp. 521–535, Oct. 1986.
[10] V. Rizzoli *et al.*, "User-oriented software package for the analysis and optimization of nonlinear microwave circuits," *Proc. Inst. Elec. Eng.*, vol. 133, pt. H, pp. 385–391, Oct. 1986.
[11] K. S. Kundert, G. B. Sorkin, and A. Sangiovanni-Vincentelli, "Applying harmonic balance to almost-periodic circuits," *IEEE Trans. Microwave Theory Tech.*, vol. 36, pp. 366–378, Feb. 1988.
[12] V. Rizzoli, C. Cecchetti, and A. Lipparini, "A general-purpose program for the analysis of nonlinear microwave circuits under multitone excitation by multidimensional Fourier transform," in *Proc. 17th European Microwave Conf.* (Rome), Sept. 1987, pp. 635–640.
[13] V. Rizzoli, C. Cecchetti, and A. Lipparini, "Numerical analysis of intermodulation distortion in microwave mixers," in *1988 IEEE MTT-S Int. Microwave Symp. Dig.*, (New York), May 1988, pp. 1103–1106.
[14] U. L. Rohde, "Harmonic-balance method handles nonlinear microwave CAD problems," *Microwave J.*, pp. 203–210, Oct. 1987.
[15] C. Holmes, O. Pitzalis, and Y. Yuan, "Harmonic-balance software simulates nonlinear circuits," *Microwaves & R.F.*, pp. 141–149, Oct. 1987.
[16] M. A. Smith *et al.*, "RF nonlinear device characterization yields improved modeling accuracy," in *1986 IEEE MTT-S Int. Microwave Symp. Dig.* (Baltimore), June 1986, pp. 381–384.
[17] V. Rizzoli, C. Cecchetti, and A. Neri, "Supercomputer-aided generalized mixer analysis and optimization," in *Proc. 16th European Microwave Conf.* (Dublin), Sept. 1986, pp. 692–697.
[18] W. R. Curtice, "Nonlinear analysis of GaAs MESFET amplifiers, mixers, and distributed amplifiers using the harmonic balance technique," *IEEE Trans. Microwave Theory Tech.*, vol. MTT-35, pp. 441–447, Apr. 1987.
[19] D. Hente and R. H. Jansen, "Frequency-domain continuation method for the analysis and stability investigation of nonlinear microwave circuits," *Proc. Inst. Elec. Eng.*, vol. 133, pt. H, pp. 351–362, Oct. 1986.
[20] R. Gilmore, "Nonlinear circuit design using the modified harmonic-balance algorithm," *IEEE Trans. Microwave Theory Tech.*, vol. MTT-34, pp. 1294–1307, Dec. 1986.
[21] M. Gayral *et al.*, "The spectral balance: A general method for analysis of nonlinear microwave circuits driven by non-harmonically related generators," in *1987 IEEE MTT-S Int. Microwave Symp. Dig.* (Las Vegas), June 1987, pp. 119–121.
[22] M. S. Nakhla and J. Vlach, "A piecewise harmonic-balance technique for determination of periodic response of nonlinear systems," *IEEE Trans. Circuits Syst.*, vol. CAS-23, pp. 85–91, Feb. 1976.
[23] R. H. Jansen, R. G. Arnold, and I. G. Eddison, "A comprehensive CAD approach to the design of MMICs up to mm-wave frequencies," *IEEE Trans. Microwave Theory Tech.*, vol. 36, pp. 208–219, Feb. 1988.
[24] K. C. Gupta, R. Garg, and R. Chadha, *Computer-Aided Design of Microwave Circuits.* Dedham, MA: Artech House, 1981.
[25] A. Madjar and F. J. Rosenbaum, "A large-signal model for the GaAs MESFET," *IEEE Trans. Microwave Theory Tech.*, vol. MTT-29, pp. 781–788, Aug. 1981.
[26] R. G. Hicks and P. J. Khan, "Numerical analysis of nonlinear solid-state device excitation in microwave circuits," *IEEE Trans. Microwave Theory Tech.*, vol. MTT-30, pp. 251–259, Mar. 1982.
[27] H. Wacker, *Continuation Methods.* New York: Academic Press, 1978.
[28] R. Fletcher, "A new approach to variable metric algorithms," *Computer J.*, vol. 13, pp. 317–322, Aug. 1970.
[29] J. W. Bandler and S. H. Chen, "Circuit optimization: The state of the art," *IEEE Trans. Microwave Theory Tech.*, vol. 36, pp. 424–443, Feb. 1988.
[30] A. Nobile and V. Roberto, "MFFT: A package for two- and three-dimensional vectorized discrete Fourier transformation," International School for Advanced Studies, Trieste, 1986.
[31] K. B. Niclas and B. A. Tucker, "On noise in distributed amplifiers at microwave frequencies," *IEEE Trans. Microwave Theory Tech.*, vol. MTT-31, pp. 661–668, Aug. 1983.
[32] A. Materka and T. Kacprzak, "Computer calculation of large-signal GaAs FET amplifier characteristics," *IEEE Trans. Microwave Theory Tech.*, vol. MTT-33, pp. 129–135, Feb. 1985.
[33] R. H. Jansen, "The spectral-domain approach for microwave integrated circuits," *IEEE Trans. Microwave Theory Tech.*, vol. MTT-33, pp. 1043–1056, Oct. 1985.
[34] R. J. Gilmore and F. J. Rosenbaum, "An analytic approach to optimum oscillator design using S-parameters," *IEEE Trans. Microwave Theory Tech.*, vol. MTT-31, pp. 633–639, Aug. 1983.
[35] Y. Xuan and C. M. Snowden, "A generalized approach to the design of microwave oscillators," *IEEE Trans. Microwave Theory Tech.*, vol. MTT-35, pp. 1340–1347, Dec. 1987.
[36] S. R. Mazumder and P. D. van der Puije, "Two-signal method for measuring the large-signal S-parameters of transistors," *IEEE Trans. Microwave Theory Tech.*, vol. MTT-26, pp. 417–420, June 1978.
[37] S. E. Sussman-Fort, S. Narasimhan, and K. Mayaran, "A complete GaAs MESFET computer model for SPICE," *IEEE Trans. Microwave Theory Tech.*, vol. MTT-32, pp. 471–473, Apr. 1984.
[38] V. Rizzoli, A. Lipparini, and F. Mastri, "Computation of large-signal S-parameters by harmonic-balance techniques," *Electron. Lett.*, vol. 24, pp. 329–330, Mar. 1988.
[39] R. A. Pucel, D. Massé, and R. Bera, "Performance of GaAs MESFET mixers at X band," *IEEE Trans. Microwave Theory Tech.*, vol. MTT-24, pp. 351–360, June 1976.
[40] E. F. Beane, "Prediction of mixer intermodulation levels as function of local-oscillator power," *IEEE Trans. Electromagn. Compat.*, vol. EMC-13, pp. 56–63, May 1971.
[41] R. G. Meyer, "Intermodulation in high-frequency bipolar transistor integrated-circuit mixers," *IEEE J. Solid-State Circuits*, vol. SC-21, pp. 534–537, Aug. 1986.
[42] S. A. Maas, "Two-tone intermodulation in diode mixers," *IEEE Trans. Microwave Theory Tech.*, vol. MTT-35, pp. 307–314, Mar. 1987.

Vittorio Rizzoli (M'79) was born in Bologna, Italy, in 1949. He graduated from the School of Engineering, University of Bologna, in July 1971.

From 1971 to 1973, he was with the Centro Onde Millimetriche of Fondazione Ugo Bordoni, Pontecchio Marconi, Italy, where he was involved in research on millimeter-waveguide communication systems. In 1973, he was with the Hewlett-Packard Company, Palo Alto, CA, working in the areas of MIC and microwave power devices. From 1974 to 1979, he was an Associate Professor at the University of Bologna, teaching a course on microwave integrate circuits. In 1980, he joined the University of Bologna as a Full Professor of Electromagnetic Fields and Circuits. His current research interests are in the fields of MIC and MMIC, with special emphasis on nonlinear circuits. He is also heading a research project aimed at the development of vectorized software for microwave circuit design applications.

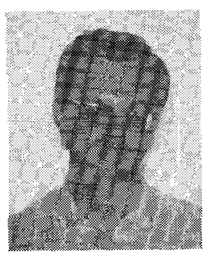

Claudio Cecchetti was born in Forlì, Italy, in 1957. He graduated in electronic engineering from the University of Bologna in October 1983.

In 1984 and early 1985 he obtained a research grant issued by Fondazione G. Marconi, Pontecchio Marconi, Italy, to develop user-friendly interactive software for linear microwave circuits CAD. In 1985, he joined Fondazione U. Bordoni, Rome, Italy, where he is currently involved in research on nonlinear microwave circuits design. His main field of interest is the development of vectorized software for MIC and MMIC design applications.

Alessandro Lipparini was born in Bologna, Italy, on August 31, 1947. He graduated with a degree in electronic engineering from the University of Bologna, Bologna, Italy, in 1974.

In 1974, he joined the Technical Staff of the Istituto di Elettronica, University of Bologna, as a Research Fellow. Since March 1975, he has been a Researcher for the Italian Ministry of Education at the University of Bologna, also serving as a Lecturer on Circuit Theory and Electromagnetic Field Theory. In 1987 he joined the University of Bologna as an Associate Professor of Electromagnetic Fields and Circuits. Since then, he has been teaching a course on microwave integrated circuits. His current research interests are in the fields of MIC and MMIC with special emphasis on nonlinear circuits. He is also involved in a research project aimed at the development of vectorized software for microwave circuit design applications.

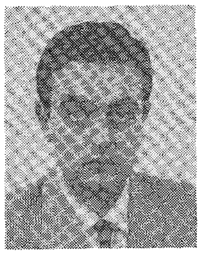

Franco Mastri was born in Forlì, Italy, in 1957. He graduated in electronic engineering from the University of Bologna in 1985.

In 1987 and 1988 he obtained research grants issued by Fondazione G. Marconi, Pontecchio Marconi, Italy, and Selenia S.p.A., Rome, Italy to carry out a study on the application of nonlinear CAD techniques in MIC and MMIC design. His research activity is mainly devoted to nonlinear microwave devices modeling and characterization and to the development of software tools for microwave circuit design.